1990 SCA CONFERENCE PAPER NUMBER 90001

Physical Relevance of Pore Types Derived From Thin Section by Petrographic Image Analysis

Robert Ehrlich and Edward L. Etris
Department of Geological Sciences

Sterling James Crabtree, Jr.
Department of Computer Science
University of South Carolina
Columbia South Carolina, 29208

June 4, 1990

consequence of the same reason, or is controlled by thermodynamic factors affecting the pore surface area of a recrystallized rock. To a first approximation, the coordination of all macropores is likely the same. If so, then the number of pore throats per unit volume will be proportional to the number of pores per unit volume. In this case, holding both porosity and capillary properties constant, the rock with the smaller sized pores will be the more permeable. This arises because the greater abundance of smaller pores results in greater numbers of pore throats.

Transmissivity is not the only property affected by relationships between pores and throats. The ratio between pore size to throat size ("aspect ratio") will be smaller in the case of the smaller pores, holding throat size constant. A smaller aspect ratio translates into more efficient expulsion of the non-wetting phase during imbibition. Quantification of pore characteristics allow determination of this ratio for each size class of pores (figure 1).

Our understanding of the porous microstructure would be advanced if the relationships between pores and throats could be quantified. In order to do so, we must first determine the numbers of pores of various sizes, and then combine this data with throat size information.

PETROGRAPHIC IMAGE ANALYSIS

The size, shape and relative proportions of pores of different types can be derived from analysis of porosity exposed in section using a procedure that we term "petrographic image analysis" ("PIA"). Such analysis is concerned with porosity exposed on a plane of section--often a petrographic thin section.

Conventional image analytic procedures result in a set of variables derived from each field of view. Calculation of these variables and simple statistics (means, standard deviations, quartiles) is often the result of such analysis. The relative proportion of porosity and the total pore perimeter are two such variables (Kendall and Moran, 1963). Other conventional variables measure aspects of size and shape of patches of porosity (Rink, 1976). In these methods, however, size and shape can only be measured if the object is entirely within the field of view. Consequently, many conventional schemes exclude objects intersected by

the frame boundary. In many cases this leads to serious and uncorrectable bias. Aside from this bias, the sizes and shapes of patches of porosity are representative of pores only in a complex geometrical-statistical manner which precludes the use of simple statistics as data summaries. The aim of petrographic image analysis is to measure and analyze porosity appropriately in order to derive unbiassed estimates of the sizes and shapes of the pores in a sample.

Pores are three dimensional objects, and so neither the size nor the shape of a pore can be observed directly from visual observation of the plane of section. To distinguish true three dimensional pores from sectioned representations in the plane of section, we define the term "porel" (porosity element). The patches of porosity exposed in section and identified and measured by image analysis are porels (figure 2). The sizes and shapes of porels are related to the sizes and shapes of pores by complex rules of geometrical probability (Kendall and Moran, 1963; Wicksell, 1925, 1926). Some porels represent sections through single pores; others represent sections through many pores connected by throats like beads on a string. Small porels may represent micropores, the tips of large pores, or even the intersection of the plane with a pore throat. Statistical procedures are necessary to determine which porels in which proportions are associated with each type of pore.

Given a collection of pores of constant size and shape, the sectioned representations will not only vary in size but also shape. A collection of equal sized cubes, for instance, will produce various sizes and shapes of triangles, parallelograms, rectangles and hexagons in the plane of section. Note that such a collection has a variance of zero in three dimensions, but is highly variable in the plane of section. Hence, conventional statistics from the plane of section will paint a much more complex picture of the porosity compared to the three dimensional reality.

Characterization of Porels of Variable Size and Shape

Pores occur in a variety of sizes and shapes (Schmidt and McDonald (1979a, 1979b); Choquette and Pray (1970); Wardlaw and Taylor (1976); Swanson (1979)). In that context, more than one distinctly different kind

of pore is intersected in most thin sections. All pores with the same size and shape are represented by a characteristic frequency distribution of porels in the plane of section (figure 3). The frequency distribution of all the sizes and shape of porels in a plane of section thus consists of mixtures of sub-distributions, each representing a different three dimensional pore type. The objective of PIA is to measure the size/shape frequency distribution in the plane of section, and then to detect the sub-distributions.

The first task toward that goal is to measure precisely the size and shape of each porel in 15 to 30 fields of view per section (figure 4). Because porel size and shape may both vary, simple measurements of conventional image analysis are insufficient.

Erosion-Dilation Differencing

The "erosion dilation differencing" porel processing procedure (Ehrlich et al., 1984; Crabtree et al., in press) was designed to precisely characterize porels of varied and potentially complex geometries, and to provide optimal input into a pattern recognition-classification algorithm for deriving pore types from the porel size/shape distributions.

"Erosion" is an operation that strips the outermost layer of pixels from a digitized porel (Crabtree et al., in press). "Dilation" is a process that adds a layer of pixels to a porel. Erosion followed by dilation will not necessarily restore the object to its original shape (Duda and Hart, 1973). The restored porel is generally smoother and contains fewer pixels than the original (figure 5). The difference in the number of pixels before and after a cycle of erosion and dilation represents the amount of small scale roughness elements present on a porel.

Two successive erosions will remove two layers of pixels, and can be followed by two successive dilations. This defines a two cycle erosion-dilation operation. The difference, compared to the original, in the number of pixels in the dilated porel after a two cycle erosion-dilation operation will be those elements involved in roughness up to four pixels wide. As erosion-dilation cycles progress (three erosions followed by three dilations, etc.), the porel is progressively smoothed until a high enough cycle of erosion exceeds the width the porel; which then is

destroyed leaving no remnant upon which an ensuing dilation can operate. The last dilation (subsequent to the erosion which completely destroys the porel) produces the smoothest component of the porel and is defined by us as the smooth component of the porel. The combined frequency distribution containing the smooth and rough component of a porel is termed a porel smooth/rough spectrum (Ehrlich et al., 1984, 1990a; Crabtree et al., in press) (figure 6b). This frequency distribution is divided into a "smooth" component (one per porel) and a "rough" component. The rough portion generally fills over many class intervals and represents pixels progressively lost over the erosion-dilation cycles.

Generally, the more complex and extensive the porel, the greater the ratio of rough to smooth pixels (figures 6a and 7). A compact porel whose shape represents the pixel equivalent of a circle will lose no pixels during erosion-dilation cycles until erosion equals the radius. On the other hand, in highly permeable reservoirs, porels may represent connected chains of pores. In that case, the smooth component (tied to the largest pore in the chain) will be represented by a relatively small proportion of the porosity of such a porel; the cores of the other pores in the porel will yield large scale roughness values. In addition, small scale roughness (pixels lost in the early stages of erosion-dilation) will be present and will represent the corners on the individual pores. This relation between the smooth/rough ratio and connectedness is of value in the next stage of analysis.

Because individual porels are components of frequency distributions, and only by analysis of these distributions can pore characteristics be derived, data for all porels are pooled across all fields of view resulting in a single smooth/rough frequency distribution for each sample.

Derivation of Pores From Porels

Derivation of pore types from porels requires analysis of frequency distributions of sizes and shapes of porosity exposed in section. This cannot be done from a section through a single sample; but simultaneous analysis of a collection of frequency distributions representing a set of related samples can extract pore sizes and shape. "Related samples" are those that have had a common burial history and

a similar lithology, such as samples of sandstone from a single core or field. This common depositional and diagenetic history ensures that pores of different type will be present in variable proportions among samples. This variability produces distinctive changes in the porel erosion-dilation spectra from sample to sample (Ehrlich, et al., 1990a).

Such variability can be manifest in one of two ways: 1) pore size and shape can be simple random variables (e.g. vary according to normal, log normal or other well-known frequency distributions) characterized by a mean and variance; or 2) pores can occur as two or more subpopulations each with a characteristic size or shape, which requires identification of each subpopulation and determination of the relative proportions. These two possibilities can be distinguished on the basis of the pattern of correlations of class intervals of the spectra compared over all samples using criteria suggested by Miesch (1976) and Klovan and Miesch (1976) (see also a discussion in Evans et al., in press). In all reservoirs studied so far such analysis indicates that porosity is configured into a few (3-10) discrete types, and does not exist as simple populations--a finding consistent with the beliefs of most petrographers (see Schmidt and McDonald, 1979b, and Choquette and Pray, 1970).

Determination of the size, shape and relative proportion of each pore type requires use of an "unmixing" algorithm which derives the smooth/rough sub-spectrum associated with each pore type from the sample smooth/rough spectrum (Full et al., 1981; Ehrlich et al., 1990a). The unmixing procedure (SAWVECB) is iterative, and upon convergence produces a classification figure (a "polytope") embedded in a space of dimensionality equal to the number of pore types. The polytope itself has a dimensionality one less than the space in which it is embedded since the data are constant-sum (each spectrum sums to unity). Thus a sample set containing three pore types can be characterized by projecting the sample spectra onto a triangle (a three end member polytope). The position of each vertex defines the smooth/rough spectrum of a three-dimensional pore type, and the location of each sample with respect to the vertex provides the relative proportions of the pore types (table 1). A rock with four pore types requires the formulation of a tetrahedral polytope; higher numbers of pore types require like polytopes of higher dimensionality.

The smooth/rough spectrum of each pore type represents the frequency distribution of porels exposed on the plane of section by intersections at various levels and orientations of that pore type. Size and shape information for each pore type can be calculated from the corresponding smooth/rough end member distributions (figure 8).

The procedure for deriving pore types is iterative and sometimes does not converge. A set of ten or more samples is generally necessary. If such samples are collected to reflect the spectrum of variability of the formation, convergence does generally occur.

Visual identification of pore types is straightforward using the smooth/rough spectra of end members as a guide. Once accomplished, they can be placed in the traditional contexts of fabric position (intergranular, intragranular, moldic) and mineralogy of the pore wall. A major advantage of the method is the ability to objectively determine the presence of more than one sort of porosity of the same type, e.g. two different classes of intergranular pores.

Validation of Pore Types

Is there independent proof of the existence of these pore types? Several lines of evidence support this. Nuclear magnetic resonance (NMR) T1 relaxation time data are related to pore size. Kenyon et al. (1989) as well as work in progress have shown that the NMR T1 spectra are polymodal, indicating a corresponding polymodality of the pore size frequency distribution. The modes are located at sizes close to those predicted from PIA analysis of thin sections of end cuts of the sample plugs. Other evidence for the validity of the derived pore types arises from success in relating pore type proportions to imbibition and drainage curves and in modelling a variety of physical characteristics of the fluid filled porosity using parameters defined by PIA (McCreesh et al., 1990; Ehrlich et al., 1990a). These models require estimates of the numbers of throats per unit volume derived by the assumption of the proportionality between numbers of pores and numbers of throats. The number of pores of a given type is equal to its porosity fraction in the sample divided by the volume of a single pore of that type. If either

quantity is in error, then model values of, for example, permeability or formation factor will not be proportional to measured values.

PORE TYPES AND THROAT SIZES

The assumption of proportionality of pore number to throat number gives small comfort unless the relationship between pore type and throat size can be determined. Throat size information is not explicitly available from thin sections but is best obtained from capillary pressure measurements, preferably mercury injection curves. Both mercury injection data and PIA data can be expressed as a set of proportions: the volume fraction of porosity filling in a given pressure increment and the volume fraction of each pore type, respectively.

The relationship between pore type and throat size can be determined given a set of samples wherein the relationship is fixed but pore type proportions vary. Sets obeying these assumptions consist of those samples with a similar thermodynamic history--samples of sandstone, for instance, from a single core or a single reservoir from most oil fields. In such a suite, pore type proportions can vary in response to changes in depositional fabric and diagenetic expression, but the relationship between pore type and throat size is likely to be similar among all samples.

The information extracted is the pattern of filling of each pore type during a capillary pressure experiment. At the extremes: 1) all pore types might fill proportionately over each pressure increment, or 2) each pore type could fill in a pressure interval separate from the others. Our findings are that the latter is closer to the mark. We find that the pattern of filling of all pore types is similar in all samples in a given reservoir and that differences in physical response are almost always accompanied by changes in the pore type assemblage.

The Relationship Between Pore Type and Throat Size

From each sample set, end cuts are thin sectioned for image analysis (Ehrlich et al., 1990a) and capillary pressure curves are obtained. The pertinent data are the relative proportions of pore types and the

proportion of porosity filled in each of several pressure increments during mercury injection. Multiple regression is used to predict saturation in each pressure increment as a function of pore type proportion (McCreesh et al., 1990). This procedure yields a set of equations, one per pressure increment (table 2). In each equation, saturation is predicted as the sum of the products over all pore types of a coefficient and a pore type proportion. All coefficients are non negative and less than unity. The coefficients associated with a single pore type will, across all equations, sum to unity. These coefficients represent the degree that each pore type fills in every pressure range (figure 9).

When analyzed in this fashion, virtually all reservoirs display an association between throat size and pore type (figure 10). The association is strongest in unbioturbated rocks, both carbonate and detrital, containing little diagenetic clay (figure 10). However, even in strongly altered rocks the preference persists for pores of different type to dominate certain ranges of throat size, albeit less strongly than with unaltered rocks. Commonly, but by no means always, throat size is monotonically related to pore size.

The relationship between pore type and throat size is based on the results of regression analysis. The coefficients are essentially average values for the sample set. Most equations have high (>.85) coefficients of determination, indicating that sample to sample deviations are usually low (figure 11). Thus, the relationship between pore type and throat size is essentially invariant at field scale.

ORIGIN OF THE PORE-TYPE/THROAT-SIZE RELATIONSHIP IN SANDSTONES

The strong association between pore type and throat size is easy to explain in the case of quartz-rich detrital sandstones where the pore system is established during the time of sediment accumulation and, by virtue of the chemical and physical stability of quartz, modified incompletely during compaction and diagenesis. The most mechanically stable fabric for a granular aggregate is for the grains to be segregated by size into separate domains. This tendency is a bugaboo in many industrial situations. Medications containing mixtures of ingredients

can, for instance, unmix into layers of separate ingredients during processing if any size difference exists between components. The action of water in the depositional environment always produces laminations of various scale. Bioturbation can destroy these structures but will produce new grain size segregates.

Segregation by any means is not complete, however, and the resulting sediment is a mosaic of well sorted, efficiently packed domains. In many cases elongate oversized pores occur at boundaries between domains. A large proportion of the total grain size variance of a sedimentary deposit arises from the domain level (Ehrlich, 1964). The distribution of sizes available and the parameters of each process generating this domainal structure define the size geometry and internal character of domains. The contrast between domains is limited by the range of sizes available at the local site of deposition. In consequence, most sands consist of a repetition of a few sorts of domains in terms of the size and sorting of constituent particles. Work in progress (Prince and Ehrlich, in preparation) involving analysis of double Fourier transforms of thin section porosity images shows that grains within domains approach ideal packing, but the domains themselves are distributed randomly.

This non-random fabric will produce a strong relationship between pore type and throat size if the domains are large with respect to the volume of a sample. In sandstones such domains may extend for several centimeters, and may be in contact with others of like sort, providing relatively great continuity with respect to the size of an average core sample. Commonly, domains are lens- or sheet-like, parallel to subparallel to bedding. Both pore type and throat size are determined by the internal (grain size and sorting) and external (size, shape and arrangement) properties of the domains.

In such fabrics there is a strong tendency for pores of the same type to be mutually adjacent. This is required to explain the relationship between pore type and throat size for many sandstones such as "Jurassic I" where the largest pore type fills almost entirely and alone in the lowest pressure interval (figure 10).

Disruption of the Depositional Fabric

Depositional factors permanently fix the locations of intergranular pores in the porosity network and, except for total cementation, those locations are unchanged during compaction and diagenesis. Modification of the porous network must be largely due to changes in pore throats. Cementation alone is not sufficient. Development of quartz overgrowths reduces pore and throat size but maintains a strong relationship between pore type and throat size.

Bioturbation, patchy carbonate cement and diagenetic clay tend to weaken the relationship between pore type and throat size (figure 10) by reducing the size of domains containing chains of pores connected by large throats. However, we have not observed such disruption gone to completion. Instead, some semblance of the original relationship persists (figure 10).

CARBONATES

A strong relationship between pore type and throat size is expected in the case of weakly cemented carbonates carrying their original depositional fabric (Etris et al., 1988) (figure 10). However, such relationships exist even in strongly recrystallized dolomites such as those from the Reinecke Field (figure 10). In such rocks we cannot call upon size sorting of the depositional fabric to produce this. Apparently, surface energy considerations in such rocks also produce this pattern. The persistence of this relationship partially accounts for the efficient production of such rocks.

SAMPLE SUPPORT

We have found that the relationship between pore type and throat size is a fixed one for any given field. Variability in permeability and other properties is strongly related to changes in the proportion of pore types. This effect is due to the presence of domains wherein pores of the same type tend to be mutually adjacent (forming laminae for example). For sandstones especially, this condition is pervasive, and so pore type

domains represent a distinct level in the hierarchy of reservoir heterogeneity.

The existence of domains means that the physical size of a sample may affect the values of properties measured from that sample. This is the cause for significantly different values of permeability and capillary pressure data from adjacent samples. This disparity occurs when the size of the sample is small in terms of the size of the elements of the mosaics. We have observed that thin sections cut from the ends of one inch plugs of sandstones commonly contain two to ten laminae or, in the case of bioturbated sands, curd-like domains (Etris, 1987). A slight shift in the sample location of a one inch plug will change the proportions of, say, laminae supporting high permeability values. At some scale of sample, repeated sampling will result in minimal variability between measurements.

This aspect of sampling has been long recognized by the mining profession, where the scale of sampling is known as the sample "support" (David, 1977). The practice in the mining industry is to physically homogenize lengths of core or channel samples and assay splits of the homogenized sample. This cannot be done in the case of permeable media because geometrical arrangement is a major control on many physical properties. Samples of a size appropriate for unbiassed measurement may be too large to be measured for economic or operational reasons. Mercury injection, for instance, must be a quasi-static procedure; the use of samples of large volume makes this assumption difficult to impossible to attain.

However, there is no practical limit to the volume sampled by PIA to derive pore type proportions. Conventional petrographic thin sections are sufficient but not necessary; impregnated slabs can be analyzed using, for instance, the reflected light fluorescence technique described by Ruzyla and Jezek (1987). It is necessary to analyze only enough conventionally sized samples so as to firmly establish a pore classification and a relationship with throat size. Physical measurements can be obtained using sample sizes appropriate for the measurement. Then the pore type proportions of a set of extended samples (each representing many centimeters of core for instance) can be used to synthesize on a large scale by modelling the physical response of a

suitable rock volume. Permeability and formation factor models have already been successfully constructed using PIA data (Ehrlich et al., in preparation). Current research indicates that resistivity index and relative permeability can also be modelled (Etris et al., in preparation).

SUMMARY AND CONCLUSIONS

The physical response of a reservoir can be affected by heterogeneities at all scales. The goal of core analysis is firstly to measure and understand phenomena at small scales, and secondly to predict response at larger scales. Many properties are strongly affected by the topology of the porous microstructure which, by virtue of capillary contrasts, restricts flow to a small portion of the microstructure (Swanson, 1979), and largely controls the localization of residual non-wetting phases at the pore level. Petrographic image analysis is one of the few procedures designed to provide direct, physically relevant measurements of a portion of the microstructural geometry: e.g. unbiassed pore information. PIA analysis shows objectively and quantitatively that, consonant with general petrographic assumptions, pores in any reservoir occur as a few (3-10) types, each type having a distinct three dimensional size and/or shape. Pore types are important because of the tendency for pores of a like type to be situated next to one another forming a mosaic of domains. A consequence of the mosaic structure is that pores of a given type tend to be linked by throats of a characteristic size. This effect is strong enough that the presence or absence of a pore type can have profound effects on fluid or electrical transmissivity.

PIA does not provide such information independently of other core analysis. Instead, it is best used in conjunction with a throat-sensitive physical test. In essence, three dimensional information is acquired by analyzing the constraints contributed by both. The relationship between pore type and throat size is determined by relating pore type proportion with mercury injection data. Data derived from this relationship is sufficient to model such single phase properties as permeability and formation factor. In a similar fashion, pore type proportions can be linked to the mercury withdrawal (imbibition) curve, indicating a strategy

for modelling relative permeability and resistivity index under various assumptions of the wetting state of the microstructure.

Pores of different type can be visually recognized using the end-member smooth/rough spectra as a guide. In this way pore wall mineralogy and the nature of the mosaics can be determined.

These results show that a strategy of reservoir description involving pore types is guaranteed to be physically relevant. Because pore type determination is the product of an explicit numerical procedure, pore type classification and measurement is not hobbled by the subjectivity associated with most kinds of geological description.

REFERENCES

Choquette, P.W., and L.C. Pray, 1970, Geologic nomenclature and classification of porosity in sedimentary rocks: AAPG Bulletin, v. 54, p. 207-250.

Crabtree, S.J., Jr., Ehrlich, R., and C. Prince, 1984, Evaluation of strategies for segmentation of blue-dyed pores in thin sections of reservoir rocks: Computer Vision, Graphics, and Image Processing, v. 28, p. 1-18.

Crabtree, S.J., Jr., Yuan, L.P., and R. Ehrlich, 1990, A fast and accurate erosion-dilation method suitable for microcomputers: CVGIP: Graphical Models and Image Processing, in press.

Crawford, G.A., Moore, G.E., and W. Simpson, 1984, Depositional and diagenetic controls on reservoir development in a Pennsylvanian phylloid algal complex: Reinecke field, Horseshoe atoll, West Texas: Transactions SW Section AAPG, p. 81-90.

David, M., 1977, Geostatistical Ore Reserve Estimation. Elsevier Scientific Publishing Company, N.Y., 364 p.

Duda, R.O., and Hart, P.E., 1973, Pattern Classification and Scene Analysis. John Wiley & Sons, N.Y., 482 p.

Ehrlich, R., 1964, The role of the homogeneous unit in sampling plans for sediments: Journal of Sedimentary Petrology, v. 34, no. 2, p. 437-439.

Ehrlich, R., Crabtree, S.J., Jr., Kennedy, S.K., and R.L. Cannon, 1984, Petrographic image analysis I--analysis of reservoir pore complexes: Jour. Sed. Pet., v. 54, no. 4, p. 1365-1378.

Ehrlich, R., Crabtree, S.J., Jr., Horkowitz, K.O., and J.P. Horkowitz, 1990a, Objective classification of reservoir porosity--petrographic image analysis I: AAPG Bulletin, in press.

Ehrlich, R., Etris, E.L., Yuan, L.P., and D.S. Brumfield, 1990b, Reservoir Petrography and Physical Models of Permeability and Formation Factor--petrographic image analysis III: AAPG Bulletin, in preparation.

Etris, E.L., 1987, Quantitative analysis of variation and distribution of porosity, pore types, and permeability in microstratified sandstone petroleum reservoirs: unpublished Master's thesis, The University of South Carolina.

Etris, E.L., Brumfield, D.S., Ehrlich, R., and S.J. Crabtree, Jr., 1988, Relations Between Pores, Throats and Permeability: A Petrographic/Physical Analysis of Some Carbonate Grainstones and Packstones: Carbonates and Evaporites, v. 3, no. 1, p. 17–32.

Etris, E.L., Ehrlich, R., and S.J. Crabtree, Jr., 1990, The relationship between pore type and throat size: consequences for resistivity index and relative permeability--petrographic image analysis IV: AAPG Bulletin, in preparation.

Evans, J.C., Ehrlich, R., Krantz, D., and W.E. Full, 1990, A comparison between polytopic vector analysis and empirical orthogonal function analysis for analyzing quasigeostrophic potential vorticity: J. Geophys. Res. Oceans, in preparation.

Full, W.E., Ehrlich, R., and J.C. Bezdek, 1982, FUZZY QMODEL--a new approach for linear unmixing: Mathematical Geology, v. 14, p. 259–270.

Full, W.E., Ehrlich, R., and J.E. Klovan, 1981, EXTENDED QMODEL--objective definition of external end members in the analysis of mixtures: Mathematical Geology, v. 13, no. 4, p. 331–344.

Kendall, M.G., and P.A.P Moran, 1963, Geometrical Probability. Hafner Publishing Company, N.Y., 125 p.

Kenyon, W.E., Howard, J.J., Sezginer, A., Straley, C., Matteson, A., Horkowitz, K.O., and R. Ehrlich, 1989, Pore-size distribution and NMR in microporous cherty sandstones. Proceedings of the Society of Professional Well Log Analysts 30th Annual Logging Symposium, Denver, Colorado, June 11–14, 1989.

Klovan, J.E., and A.T. Miesch, 1976, EXTENDED CABFAC and QMODEL computer programs for Q-mode factor analysis of compositional data: Comput. Geosci., v. 1, p. 161–178.

Matheron, G., 1967, Elements Pour Une Theorie Des Milieux Poreux. Masson et Cie, Editeurs, Paris, 166 p.

McCreesh, C.A., Ehrlich, R., and S.J. Crabtree, Jr., 1990, Relating thin section porosity to capillary pressure--petrographic image analysis II: AAPG Bulletin, in press.

Miesch, A.T., 1976, Q-mode factor analysis of geochemical and petrologic data matrices with constant row-sums: U.S. Geol. Survey Prof. Paper, 574-G, 47 p.

Prince, C., and R. Ehrlich, 1990, Double Fourier analysis of thin section porosity: in preparation.

Rink, M., 1976, A computerized quantitative image analysis procedure for investigating features and an adopted image process: Jour. Microscopy, v. 107, pt. 3, p. 267-386.

Ruzyla, K., and D.I. Jezek, 1987, Staining method for recognition of pore space in thin section and polished sections: Jour. Sed. Pet., v. 57, no. 4, p. 777-778.

Schmidt, V., and D.A. McDonald, 1979a, The role of secondary porosity in the course of sandstone diagenesis: in SEPM Special Publication No. 26, Scholle, P.A., and Schluger, P.R., (Eds.), p. 175-207.

Schmidt, V., and D.A. McDonald, 1979b, Texture and recognition of secondary porosity in sandstones: in SEPM Special Publication No. 26, Scholle, P.A., and Schluger, P.R., (Eds.), p. 209-225.

Swanson, B.F., 1979, Visualizing pores and nonwetting phase in porous rock: Journal of Petroleum Technology, (Jan. 1979), p. 10-18.

Wardlaw, N.C., and R.P. Taylor, 1976, Mercury capillary pressure curves and the interpretation of pore structure and capillary behavior in reservoir rocks: Bulletin of Canadian Petroleum Geology, v. 24, p. 225-262.

Wicksell, S.D., 1925, The corpuscle problem. A mathematical study of a biometric problem: Biometrika, v. 17, p. 84-99.

Wicksell, S.D., 1926, The corpuscle problem. Second memoir. Case of ellipsoidal corpuscles: Biometrika, v. 18, p. 152-172.

Table 1

Benoist Sandstone

Pore-Type Spectra

Interval Width (um)		PT1	PT2	PT3
Smooth	0 - 28	20.7	5.7	0.1
Smooth	29 - 40	10.5	7.2	0.5
Smooth	41 - 60	8.9	11.6	2.5
Smooth	61 - 204	0.8	12.8	20.5
Rough	0 - 12	16.8	7.2	3.4
Rough	13 - 20	15.9	10.0	4.6
Rough	21 - 28	12.4	11.0	6.6
Rough	29 - 36	7.5	10.7	7.9
Rough	37 - 48	6.3	12.5	14.0
Rough	49 - 200	0.0	11.0	39.5
Pore Width:		24.6 um	53.9 um	89.4 um

Pore-Type Proportions

SN	PT1	PT2	PT3
BST130	0.6671	0.3349	0.0000
BST132	0.2426	0.5123	0.2451
BST133	0.1407	0.5932	0.2660
BST134	0.3429	0.3740	0.2831
BST135	0.3207	0.5656	0.1137
BST136	0.8349	0.0027	0.1624
BST137	0.1568	0.6787	0.1645
BST138	0.7138	0.2067	0.0794
BST139	0.1267	0.6046	0.2687
BST140	0.0699	0.3963	0.5337
BST142	0.4721	0.4563	0.0716
BST143	0.3428	0.6013	0.0559
BST144	0.0000	0.4690	0.5310
BST145	0.0584	0.5082	0.4335
BST146	0.1568	0.0005	0.8427

Table 2

Benoist Sandstone

Prediction Equations
Determined Via Regression

Pressure Range (psi)			R^2
Sat	(0-7)	= .21 (PT2) + .23 (PT3)	.85
Sat	(8-9)	= .04 (PT2) + .25 (PT3)	.78
Sat	(10-11)	= .02 (PT2) + .52 (PT3)	.94
Sat	(12-16)	= .39 (PT2)	.91
Sat	(17-30)	= .56 (PT1) + .19 (PT2)	.89
Sat	(31-450)	= .44 (PT1) + .15 (PT2)	.95

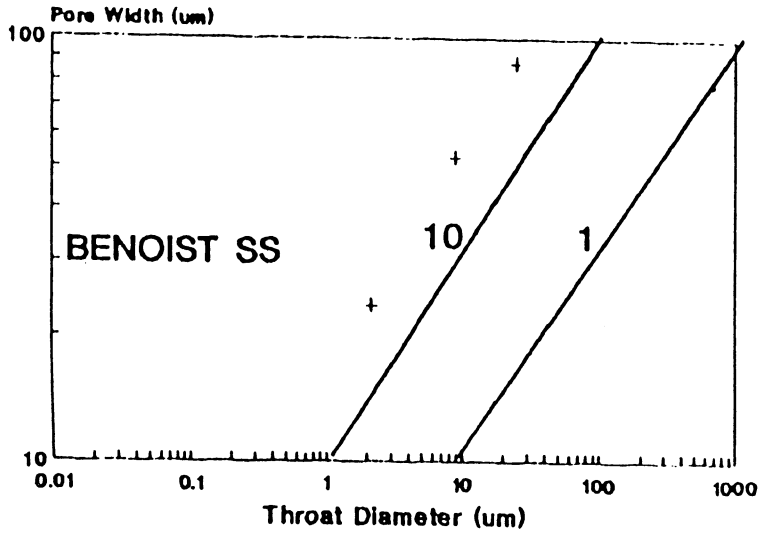

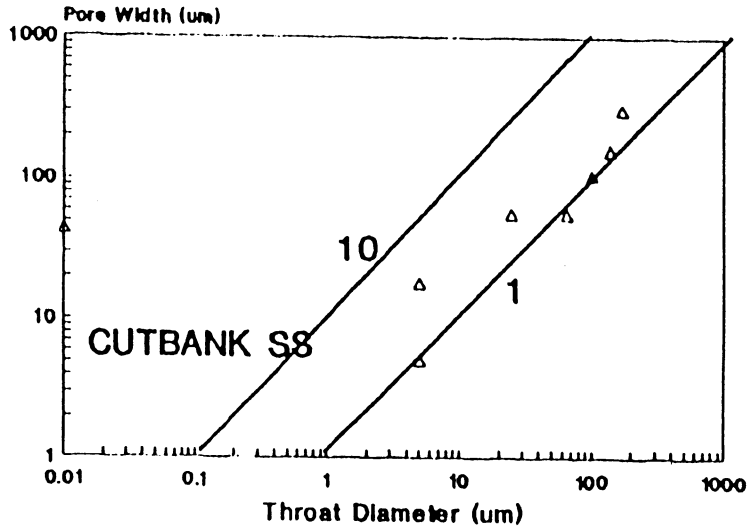

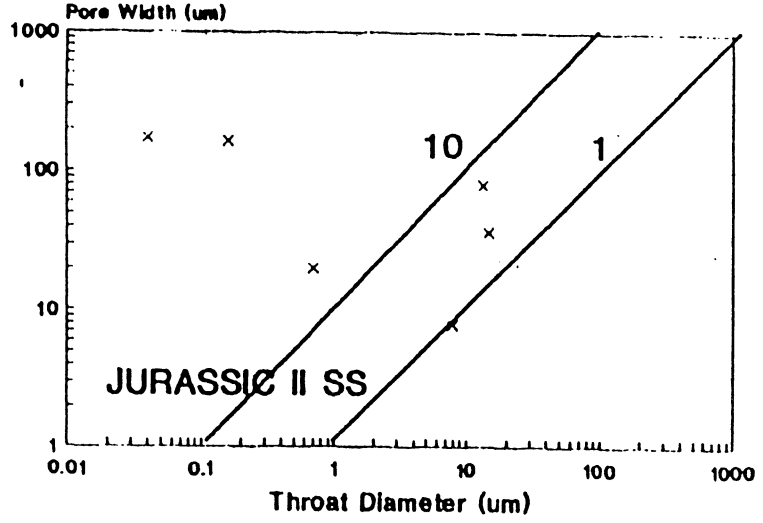

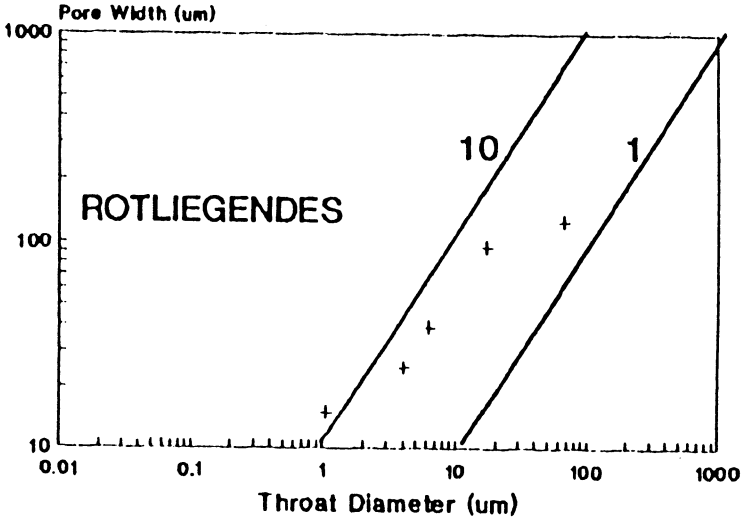

Figure 1.--Relationship between throat size and pore size for four sandstones, derived by combining thin section data with mercury porosimetry data. Diagonal lines labelled "1" and "10" represent ratios of pore size to throat size of one and ten, respectively.

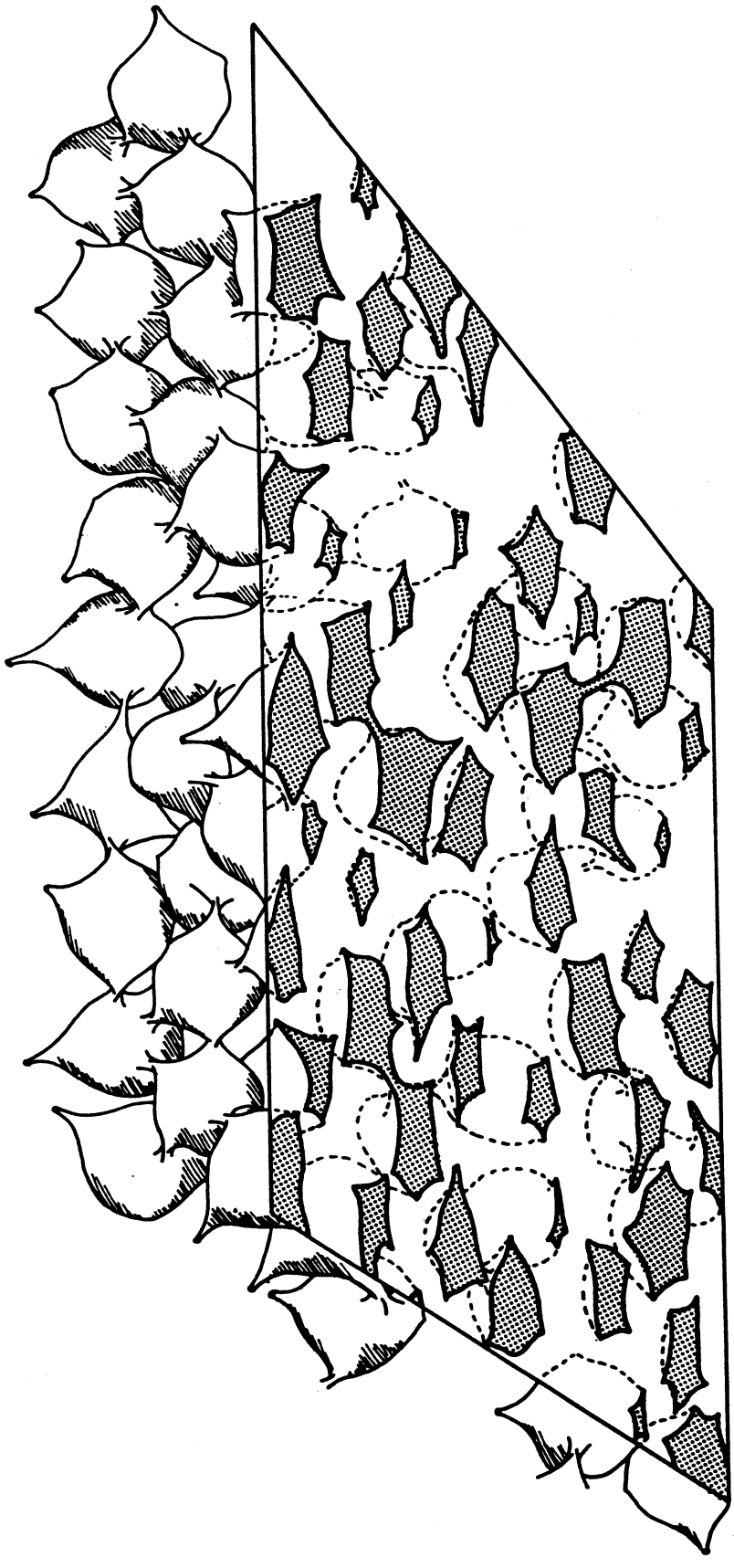

Figure 2.--Porosity exposed in a plane of section will be less well-connected and will have a greater variance in size than the pores from which they were derived.

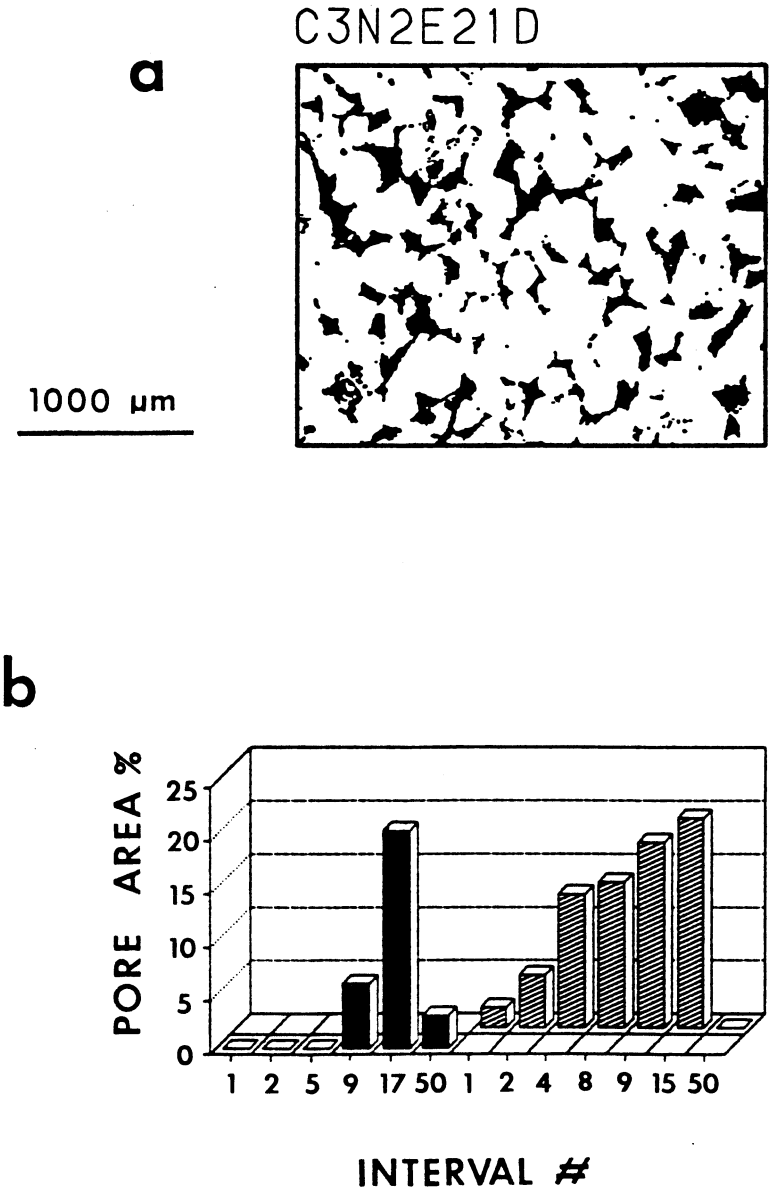

Figure 3.--A binary image (a) of porels derived from a single pore type. The erosion/dilation spectrum (b) of the pore type occurring in (a). Black bars represent the smooth component; hachured bars represent the rough component. (Modified from Ehrlich et al., 1990a.)

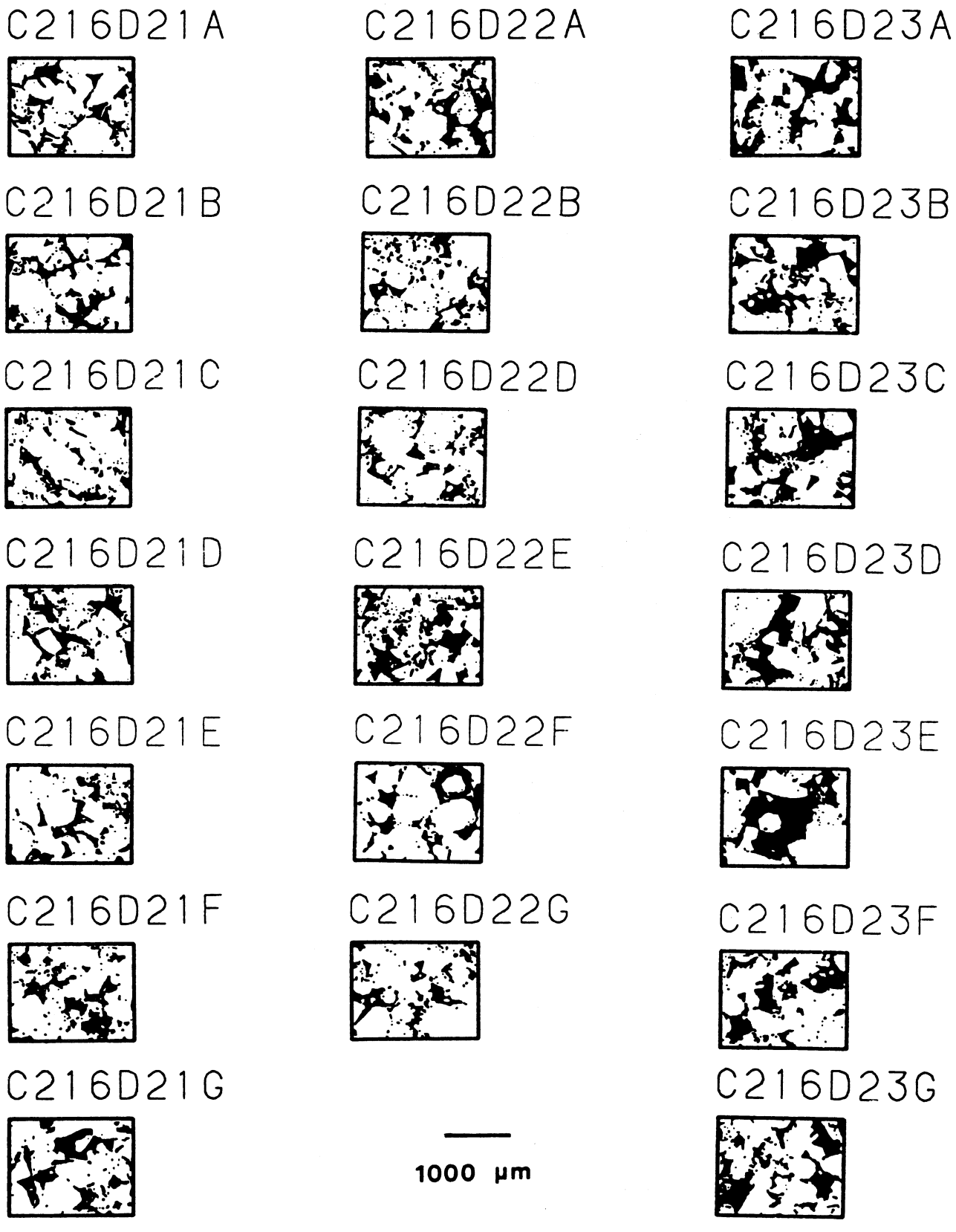

Figure 4.--Example of the variability in porosity between fields of view from a single thin section of the Cutbank Sandstone. (From Ehrlich et al., 1990a.)

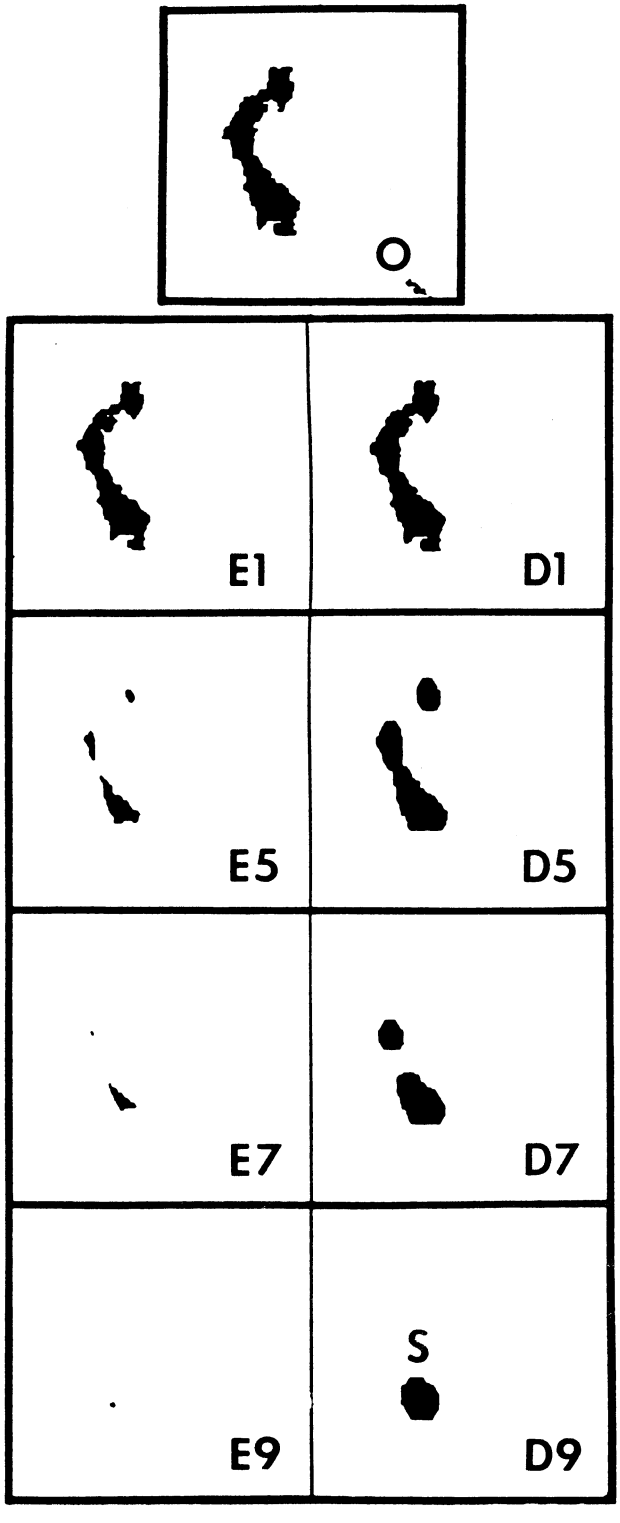

Figure 5.--Example of the progressive smoothing of a porel of simple geometry (labelled "O") during the erosion (labelled "E") and dilation (labelled "D") processes. The final dilation (D9) represents the smooth component of the porel (labelled "S"). (From Ehrlich et al., 1990a.)

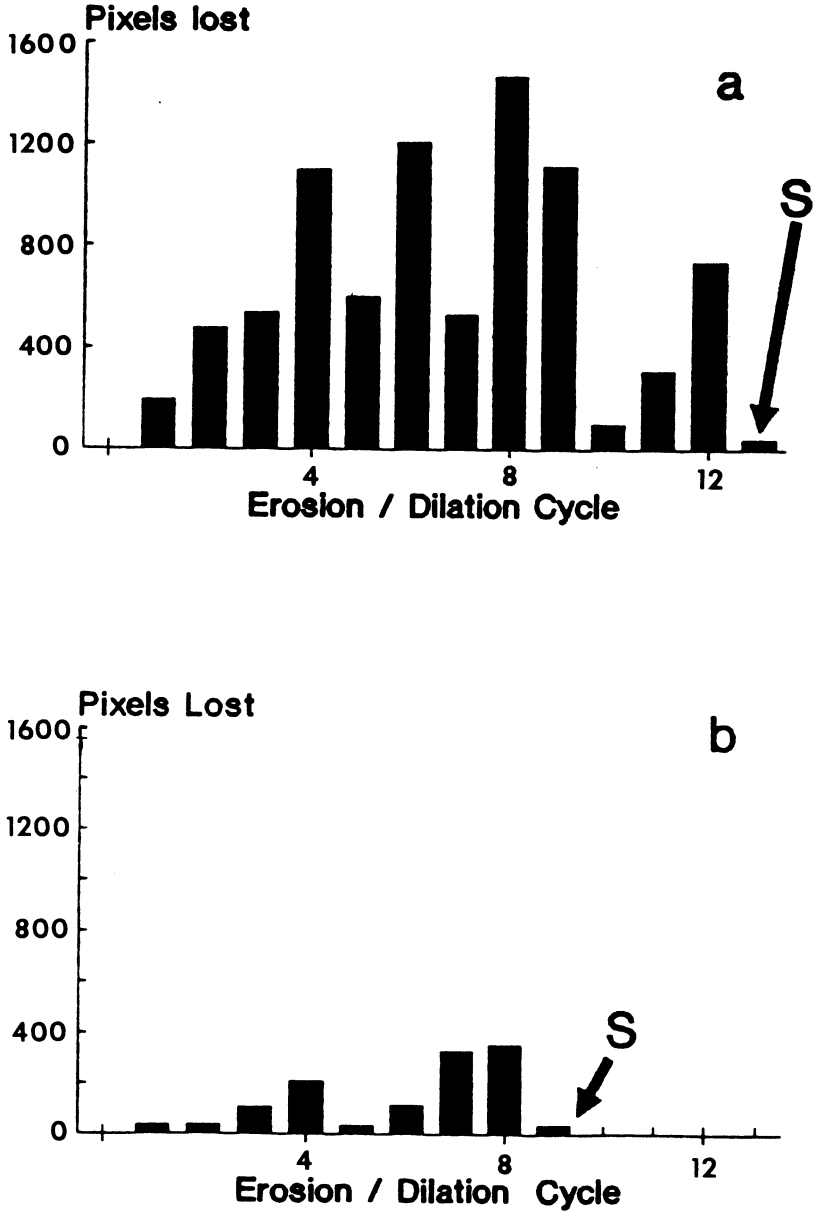

Figure 6.--Erosion/dilation spectra of two porels. The smooth component is labelled "S." (From Ehrlich et al., 1990a.)
a.-Spectrum of a large, complex porel consisting of many linked pores (see figure 7).
b.-Spectrum of a relatively small, simply shaped porel (see figure 5).

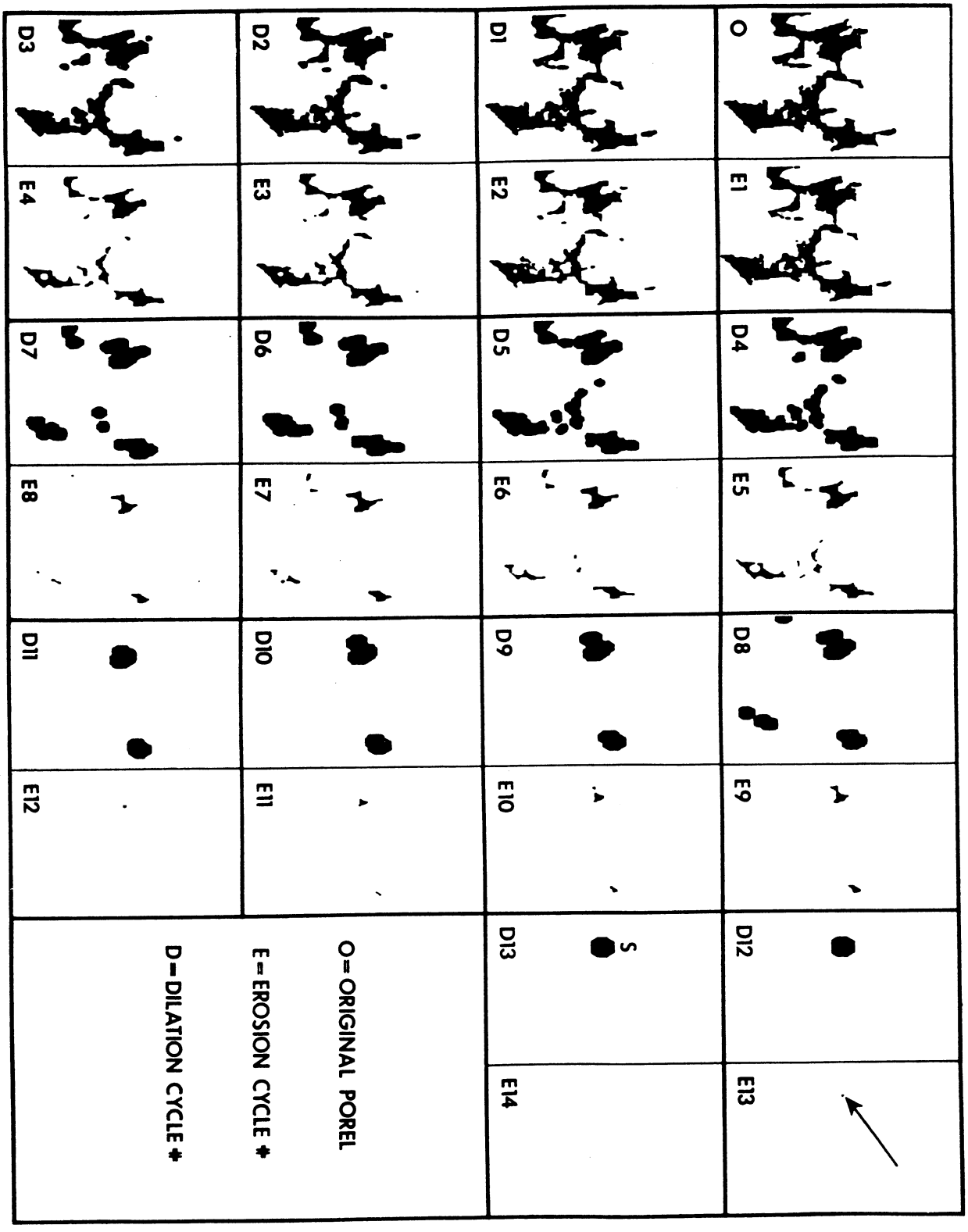

Figure 7.--Sample of the erosion/dilation process involving a complex patch of intergranular porosity. The smooth component (labelled "S" in "D13") is a small proportion of the porel. Note that the higher cycle roughness (>5) separates pore bodies. (From Ehrlich et al., 1990a.)

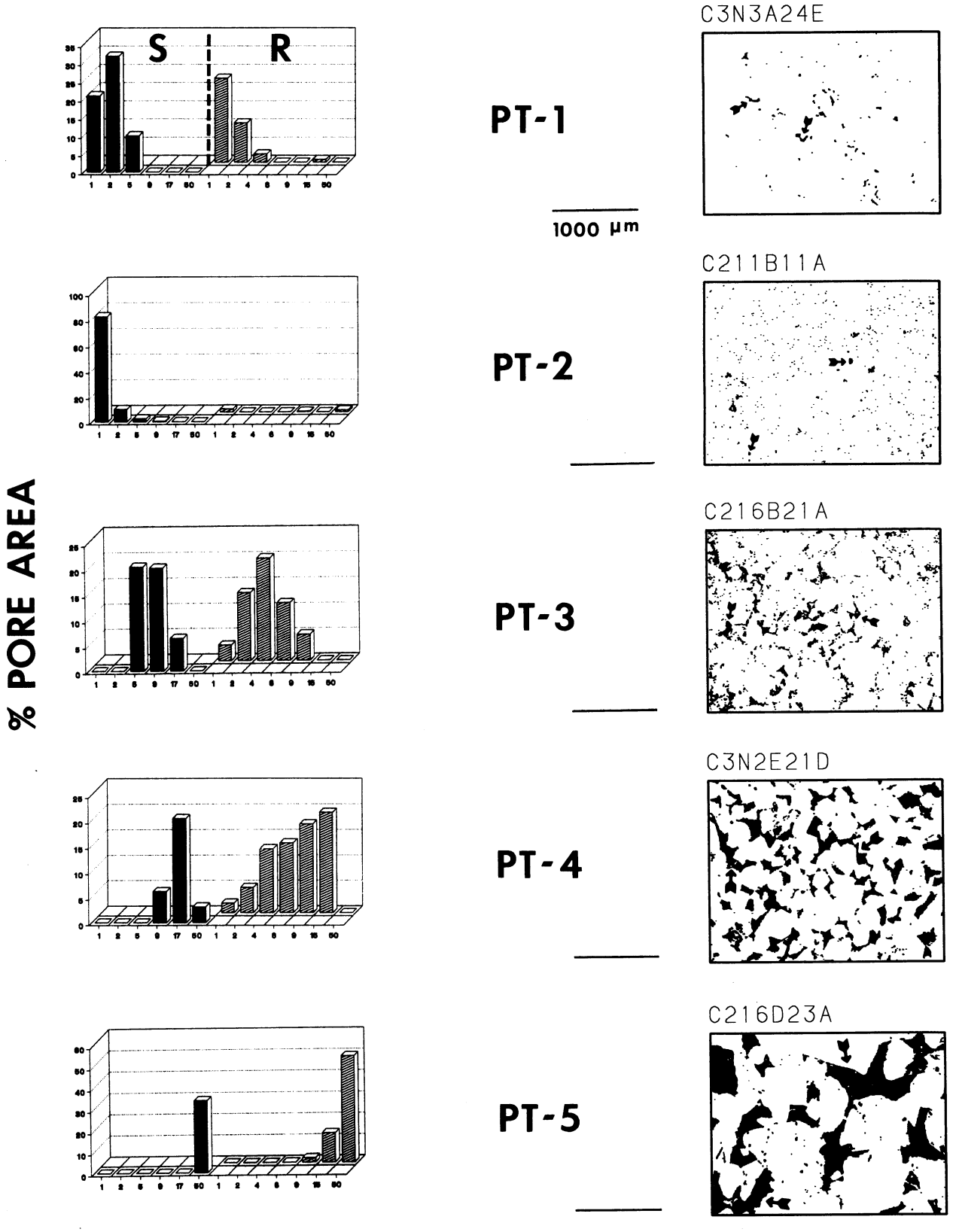

Figure 8.--Pore type spectra and representative views for the Cutbank sandstone. Pore types are, by convention, numbered in order of increasing size. (From Ehrlich et al., 1990a.)

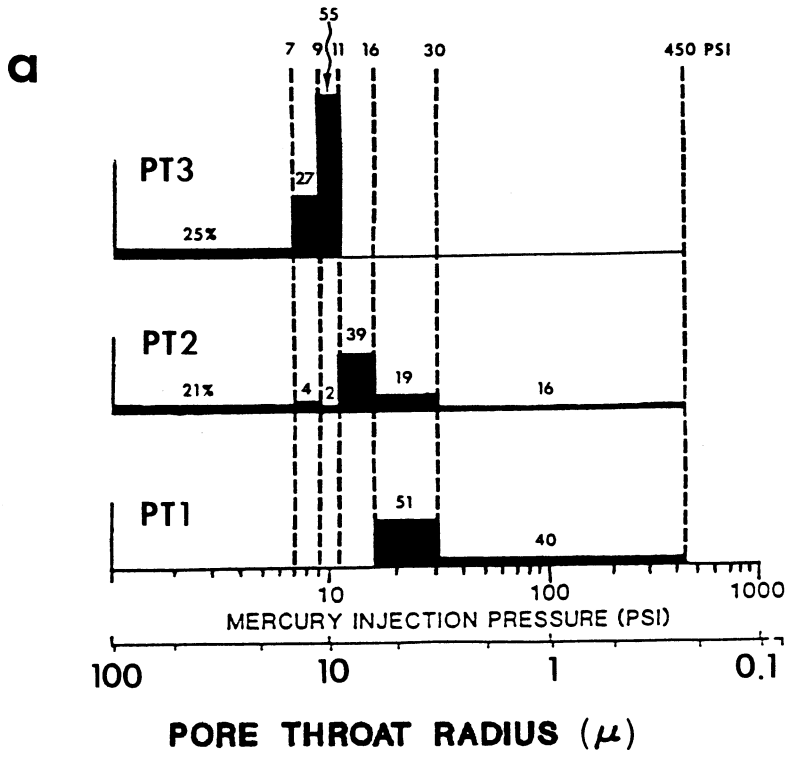

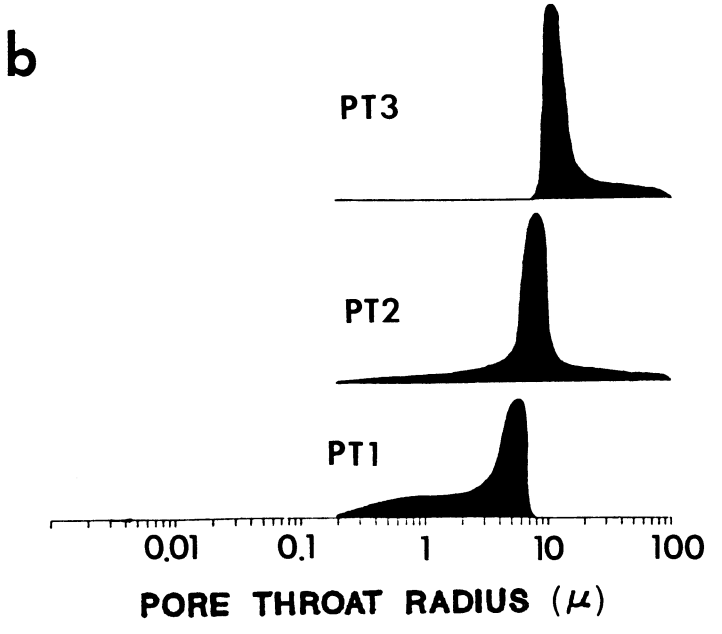

Figure 9.--Relationship between pore types and throat sizes. (Modified from McCreesh et al., 1990.)
a.-Relationship derived by regression of pore type proportions with mercury injection data. Data is expressed in terms of log mercury pressure, showing the pressure intervals used in regression. Note that pressure increases to the right.
b.-Distribution of porosity versus throat size for each pore type, derived from (a). Note that throat size increases to the right.